# NUMERICAL SIMULATION OF NEWTONIAN AND NON-NEWTONIAN FLUIDS IN CHANNEL GEOMETRIES

**Vladimír Prokop**[1], **Radka Keslerová**[1], **Karel Kozel**[1]

[1]Czech Technical University in Prague, Faculty of Mechanical Engineering,
Department of Technical Mathematics
121 35 Prague 2, Karlovo nám. 13, Czech republic

*prokop@marian.fsik.cvut.cz(Vladimír Prokop)*

**Abstract**

This paper deals with a numerical solution of laminar incompressible steady flows of Newtonian and non-Newtonian fluids. Geometrically different parts of the cardiovascular system are taken into account, for instance bifurcations of vessels or a bypass of a restricted vessel. Only channel geometries with rigid walls are used to model previously mentioned parts of the cardiovascular system. Blood flow is considered to be Newtonian in the case of vessels of large diameters as aorta. On the other hand, with decreasing diameter of a vessel the non-Newtonian behavior of blood can play a significant role. One could describe these problems using Navier-Stokes equations and continuity equation (see [1]). In the case of Newtonian fluids one considers constant viscosity compared to non-Newtonian fluids where viscosity varies and can depend on the tensor of deformation. The model used for non-Newtonian fluids is a variant of power-law. In order to find numerical solution, the system of equations is completed using artificial compressibility method. Its principle is based on addition of the time derivative of pressure divided by a specific constant into the continuity equation (see [2]). The space derivatives are discretised using the cell centered finite volume method. An arising system of ordinary differential equations is solved using explicit multistage Runge-Kutta method with given steady boundary conditions. This way one can find steady solution of unsteady system. The numerical results for two and three dimensional cases of Newtonian and non-Newtonian fluid flows in different geometries are presented and compared.

**Keywords: Finite Volume Method, Navier-Stokes equations, Newtonian fluids, Non-Newtonian fluids, Runge-Kutta method.**

**Presenting Author's Biography**

Vladimír Prokop. Postgraduate student at the Czech Technical University (CTU), Faculty of Mechanical Engineering, Department of Technical Mathematics. He achieved master degree in mechanical engineering specialization in applied mechanics at CTU in 2002. His graduation thesis was engaged in numerical solution of flows in bypass geometry. He has attended Diploma Course in the Von Karman Institute in Belgium in 2006/07.

*ISBN 978-3-901608-32-2*  

# 1 Introduction

The motivation for numerical solution of the fluid flow of Newtonian and non-Newtonian fluids arises in many applications, e.g. in the biomedicine, food industry, chemistry, glaciology etc. Many common fluids are non-Newtonian: paints, solutions of various polymers, food products. Arterial flow phenomena such as flow separation, recirculation and secondary flow motion in atherosclerotic vessels is of great interest, because these vessels present a substantial health risk and are major causes of mortality and morbidity in the industrialized word. The main points of non-Newtonian behaviour are the ability of the fluid to shear thin or shear thicken in shear flows, the presence of non-zero normal stress differences in shear flows, the ability of the fluid to yield stress, the ability of the fluid to exhibit relaxation, the ability of the fluid to creep, see [3]. When the viscosity decreases with increasing shear rate, the fluid is called shear-thinning. In the opposite case where the viscosity increases as the fluid is subjected to higher shear rate, the fluid is called shear-thickening. Experimental tests reveal that blood exhibits non-Newtonian phenomena such as shear thinning, creep and stress relaxation. In order to include all these features one can use Oldroyd-B model. Only shear thinning is considered in this work. The solution of flows in branching channels and channels with bypass is important for modelling of blood flow in arteries. The study of blood flow in large and medium arteries is a very complex task because of the heterogeneous nature of the problem and the extreme complexity of blood and arterial wall dynamics. Although blood is actually a non-Newtonian suspension of cells in plasma, it is reasonable to model it as a Newtonian fluid in vessels greater than approximately $0.5$ mm in diameter [4]. The occurring shear rates are in a range where non-Newtonian effects are only in minor significance to the flow parameters. This type of flow could be described by conservation laws of mass and momentum (Navier-Stokes equations), where the influence of exterior forces and heat exchange is not taken into account. In this case the model of a vessel is a tube with rigid walls. The pulsatile character of blood flow is not considered as well as the elasticity of arterial walls.

# 2 Mathematical model

First, one considers a non-Newtonian fluids. The non-Newtonian fluid is the fluid in which the viscosity changes with the applied shear force. As a result, the non-Newtonian fluids may not have a well-defined viscosity.

The generalized system of two dimensional Navier-Stokes equations and continuity equation for incompressible laminar flows in conservative form is written as follows

$$\tilde{R}W_t + F_x + G_y = \frac{\tilde{R}}{\mathrm{Re}}\Delta W, \qquad \tilde{R} = \mathrm{diag}\|0,1,1\|. \tag{1}$$

where the Reynolds number defined as $Re = dw^*/\nu$ in 2D and $Re = d_h w^*/\nu$ in 3D is an important parameter of the flow. Quantity $w^*$ is a characteristic velocity (the speed of upstream flows), $\nu = \eta/\rho$ is the kinematic viscosity, $d$ is a length scale (the width of the channel), $d_h = 4S/O$ is the hydraulic diameter, $S$ is the area section of the duct and $O$ is the wetted perimeter. In equation (1), $W = (p,u,v)^T$ is the vector of solution, $\tilde{R} = \mathrm{diag}\|0,1,1\|$, and $F = (u, u^2+p, uv)^T, G = (v, uv, v^2+p)^T$ denote inviscid fluxes, $(u,v)$ is the dimensionless velocity vector ($u = u^*/q_\infty$, $v = v^*/q_\infty$), $p$ denotes the dimensionless pressure ($p = p^*/\rho q_\infty^2$), $t$ is the dimensionless time ($t = t^* q_\infty/l$), and $q_\infty$ is defined as a velocity of incoming flow ($q_\infty = u^*$).

In the case of non-Newtonian fluids the power-law fluids are considered. The dominant difference from the Newtonian behaviour is shear thinning or shear thickening. From variety of power-law fluids we choose the simplest one:

$$\tau(\mathbf{e}) = 2\nu_0 |\mathbf{e}|^r \mathbf{e}, \tag{2}$$

where $\tau$ is the stress tensor, $\mathbf{e} = (e_{ij}),\ i,j = 1,2$ is the strain tensor with components $e_{11} = u_x,\ e_{12} = e_{21} = (v_x + u_y)/2,\ e_{22} = v_y,\ |\mathbf{e}|$ denotes the Euclidean norm of a tensor, $\nu_0$ is a positive constant related to the limit of generalized viscosity $\mu_g(\kappa)$ when $\kappa \to 0$, $r$ is a constant of the model. The model captures the shear thinning fluid if $r \in (-1,0)$, shear thickening fluid if $r > 0$, and $r = 0$ corresponds to the Newtonian fluid. For the non-Newtonian fluids the system of 2D Navier-Stokes equations and the continuity equation in two dimensional case written in the dimensionless conservative form reads

$$\tilde{R}W_t + F_x + G_y = \frac{\tilde{R}}{\mathrm{Re}}(R_x + S_y) \tag{3}$$

where $R = (0, g_{11}, g_{21})^T,\ S = (0, g_{12}, g_{22})^T$, $g_{ij} = 2|\mathbf{e}|^r e_{ij},\ i,j = 1,2$ and components of $e_{ij}$ defined above.

$$\begin{aligned}(g_{11})_x + (g_{12})_y &= 2|\mathbf{e}|_x^r u_x + |\mathbf{e}|_y^r (u_y + v_x) + |\mathbf{e}|^r \Delta u \\ (g_{21})_x + (g_{22})_y &= |\mathbf{e}|_x^r (u_y + v_x) + 2|\mathbf{e}|_y^r v_y + |\mathbf{e}|^r \Delta v\end{aligned} \tag{4}$$

Let us stress that subindices $_x$ and $_y$ denote partial derivatives with respect to $x$ and $y$ and that $\Delta$ stands for the 2D Laplacian. At the inlet the Dirichlet boundary condition for velocity vector $(u,v)^T$ is prescribed, at the outlet the pressure value is given. On the wall the zero Dirichlet boundary conditions for the components of velocity are used.

## 2.1 Boundary conditions

At the inlet the Dirichlet boundary condition for the velocity components $(u,v) = (q_\infty, 0)$ is prescribed and the pressure $p$ is computed by extrapolation from a domain. At the outlet the value of the pressure is prescribed by $p = p_2$, where $p_2$ is the dimensionless value of the pressure, that is higher then the initial value of the pressure at the inlet to ensure pressure gradient. The velocity components are extrapolated at the outlet. On the walls one considers the non-permeability and no-slip conditions for the velocity and the value of the pressure is taken from inside of the domain.

ISBN 978-3-901608-32-2  

## 3 Numerical solution by finite volume method

In what follows a steady state solution is considered. In such a case the artificial compressibility method can be used. The continuity equation is completed with the term $p_t/a^2$, where $a^2 > 0$. The pressure satisfies the artificial equation of state: $p = \rho/\delta$, in which $\rho$ is the artificial density, $\delta$ is the artificial compressibility, that is connected to the artificial speed of sound by relation $a = \delta^{-\frac{1}{2}}$, see [2]. Then system of governing equations has the form

$$W_t + F_x + G_y = \frac{\tilde{R}}{Re}\left(R_x + S_y\right), \tag{5}$$

where $W = (p/a^2, u, v)^T$. The equation (5) can be rewritten in the following way

$$W_t = -(\tilde{F}_x + \tilde{G}_y) \tag{6}$$

where

$$\tilde{F} = F - \frac{1}{Re}R, \tilde{G} = G - \frac{1}{Re}S \tag{7}$$

$F$ and $G$ are inviscid fluxes defined above and $R$ and $S$ are viscous fluxes representing right hand side in the case of Newtonian or non-Newtonian fluid, see also [5] and [6].

The system of equations (6) is integrated over $D_{ij}$ (finite volume cells is shown in Fig. 1). After applying mean value theorem on left hand side and Green's theorem on right hand side we get

$$W_t\mid_{ij} = -\frac{1}{\mu_{ij}}\oint_{\partial D_{ij}} \tilde{F}\mathrm{d}y - \tilde{G}\mathrm{d}x. \tag{8}$$

The integrals on the right hand side are numerically

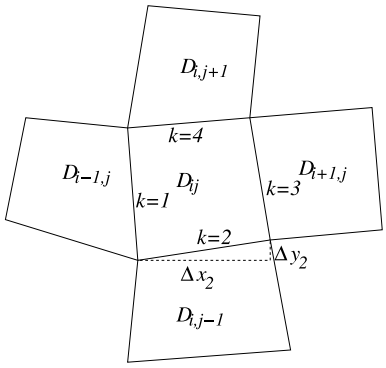


Fig. 1 Finite volume cell

approximated by

$$W_t\mid_{ij} = -\frac{1}{\mu_{ij}}\sum_{k=1}^{4}\tilde{F}_{ij,k}\Delta y_k - \tilde{G}_{ij,k}\Delta x_k. \tag{9}$$

The system of ordinary differential equations ((9)) with given steady boundary conditions is then solved by the multistage Runge-Kutta method.

$$\begin{aligned} W_{i,j}^n &= W_{i,j}^{(0)} \\ W_{i,j}^{(r)} &= W_{i,j}^{(0)} - \alpha_r \Delta t \overline{R} W_{i,j}^{(r-1)}, \quad r = 1, \ldots, m \\ W_{i,j}^{n+1} &= W_{i,j}^{(m)}, m = 3, \end{aligned}$$

where $W_{ij}^n$ denotes an approximation of $W$ at grid point $(x_i, x_j)$ and at a time $t = t_n$, $\Delta t = t_n - t_{n-1}$ is the time step, and

$$\overline{R}W_{i,j}^{(r-1)} = \tilde{R}W_{i,j}^{(r-1)} - DW_{i,j}^n.$$

The coefficients are $\alpha_1 = 0.5, \alpha_2 = 0.5, \alpha_3 = 1.0$ and the term $DW_{ij}^n$ is the artificial viscosity term of Jameson's type,see [7].

The numerical method is of the second order in time and space. The form of residual $\tilde{R}W_{i,j}^n$ depends on the method used for the space discretization, which is in this case the finite volume method in the cell centered formulation:

$$\tilde{R}W_{i,j} = \frac{1}{\mu_{ij}}\sum_{k=1}^{4}\left[\left(F_k^i - \frac{1}{Re}F_k^v\right)\Delta y_k - \left(G_k^i - \frac{1}{Re}G_k^v\right)\Delta x_k\right], \tag{10}$$

where $F^i = F, G^i = G$ are inviscid fluxes and $F^v = (0, u_x, v_x)^T, G^v = (0, u_y, v_y)^T$ are viscous fluxes, the index $k$ corresponds to the side of a finite volume. The artificial viscosity term $DW_{i,j}^n$ depends in this case on the second derivatives of the pressure and is used to improve stability of the solution. The dissipative artificial viscosity term is constructed as follows:

$$\begin{aligned} DW &= D_xW + D_yW \\ D_xW &= d_{i+\frac{1}{2},j} - d_{i-\frac{1}{2},j} \\ D_yW &= d_{i,j+\frac{1}{2}} - d_{i,j-\frac{1}{2}} \\ d_{i+\frac{1}{2},j} &= \frac{h_{i+\frac{1}{2},j}}{\Delta t}\epsilon^{(2)}_{i+\frac{1}{2},j}(W_{i+1,j} - W_{i,j}) \\ \nu_{i,j} &= \frac{|p_{i+1,j} - 2p_{i,j} + p_{i-1,j}|}{|p_{i+1,j}| + 2p_{i,j} + |p_{i-1,j}|} \\ \epsilon^{(2)}_{i+\frac{1}{2},j} &= \kappa^{(2)}\max(\nu_{i+1,j}, \nu_{i,j}), \end{aligned}$$

where $\kappa^{(2)}$ has to be chosen in order to achieve convergence of the method.

In order to satisfy the stability condition the time step is chosen as (for details see, [8]):

$$\Delta t = \min_{i,j,k}\frac{\mathrm{CFL}\ \mu_{ij}}{\rho_A\Delta y_k + \rho_B\Delta x_k + \frac{2}{\mathrm{Re}}\left(\frac{(\Delta x_k)^2 + (\Delta y_k)^2}{\mu_{ij}}\right)}, \tag{11}$$

$$\rho_A = \mid \hat{u} \mid + \sqrt{\hat{u}^2 + 1} \qquad \rho_B = \mid \hat{v} \mid + \sqrt{\hat{v}^2 + 1},$$

$\mid \hat{u} \mid, \mid \hat{v} \mid$ are the maximal values of the components of velocity vector inside the computational domain.

The computation is performed until the value of the $\mathrm{L}^2$-norm of residual satisfy Rez $W_{ij}^n \leq \epsilon_{ERR}$ with $\epsilon_{ERR}$

 

small enough ($MN$ denotes the number of grid cells in the computational domain), where

$$\text{Rez } W_{ij}^n = \sqrt{\frac{1}{MN}\sum_{ij}\left(\frac{W_{ij}^{n+1} - W_{ij}^n}{\Delta t}\right)^2}. \quad (12)$$

## 4 Numerical results

In this section we present the numerical results of Newtonian and non-Newtonian flows in different channel geometries. First, numerical results for channels with one entrance and two exit parts are presented. Figures 2 and 3 show the fluid velocity distribution for Reynolds number 1500 for Newtonian and non-Newtonian fluid in a branching channel. One can observe that the velocity profiles for non-Newtonian fluid are elongated compared to Newtonian fluid. The peak values of velocity seems to be higher for non-Newtonian fluid. The convergence history is presented. Second, numerical results for the case with splitting outlet channels is shown on figures 4 and 5 in the terms of the fluid velocity distribution for Reynolds number 1500. Again the same characteristic differences can be observed as in the previous case. Third,the three dimensional branching channel for Reynolds number 300 is shown on fig. 6 and fig. 7 for the case on non-Newtonian fluid. Fig. 6 shows axial cut in the middle of the channel while the fig. 7 shows radial cuts in the different places along the channel. In the same form are presented results for Newtonian fluid on fig. 8 and fig. 9. 3D results in the axial cut shows slight differences compared to 2D results. Fourth, fig. 10 and fig. 11 shows the fluid velocity distribution for the 3D Newtonian fluids in the splitting channel. The history of convergence of the residuals of the vector $W = (p, u, v, w)^T$ is presented. By the symbol $q$ the velocity magnitude is denoted, i.e. $q = \sqrt{u^2 + v^2 + w^2}$. Finally we present results of Newtonian fluid flow in the channel with bypass. Figures 12 and 13 show isolines of velocity in 3D for $Re = 500$. The figure 12 shows a bypass and 13 shows a main channel that represents a vessel. There is no comparism with an experiment at this moment, but the results seems to be qualitatively correct.

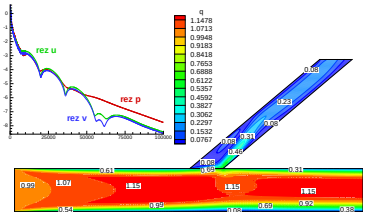


Fig. 2 Velocity isolines of 2D channel for Newtonian fluids

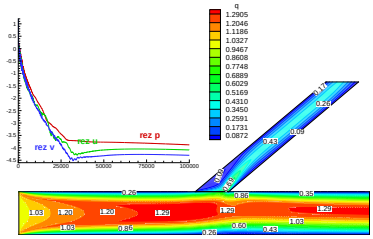


Fig. 3 Velocity isolines of 2D channel for non-Newtonian fluids

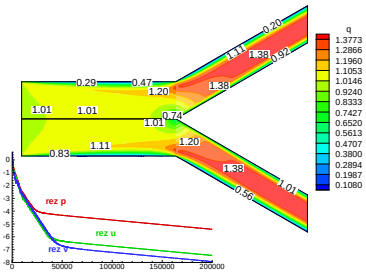


Fig. 4 Velocity isolines of 2D channel for Newtonian fluids

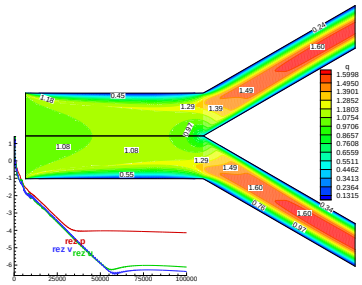


Fig. 5 Velocity isolines of 2D channel for non-Newtonian fluids

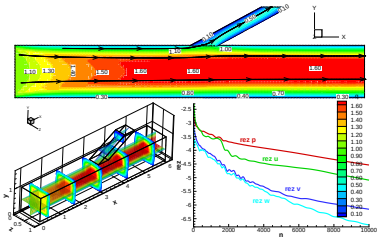


Fig. 6 Velocity isolines of 3D channel for non-Newtonian fluids

*ISBN 978-3-901608-32-2*  

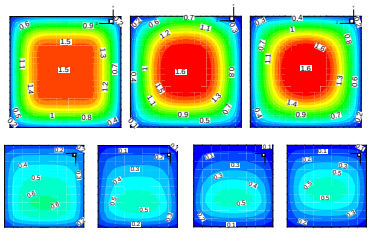

Fig. 7 Velocity isolines in the cuts of 3D channel for non-Newtonian fluids

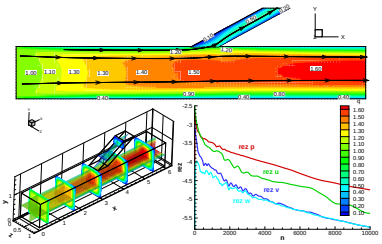


Fig. 8 Velocity isolines of 3D channel for Newtonian fluids

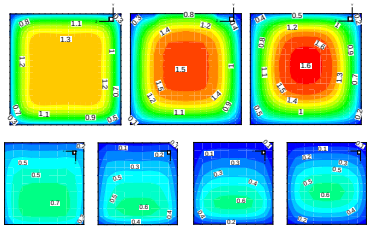

Fig. 9 Velocity isolines in the cuts of 3D channel for Newtonian fluids

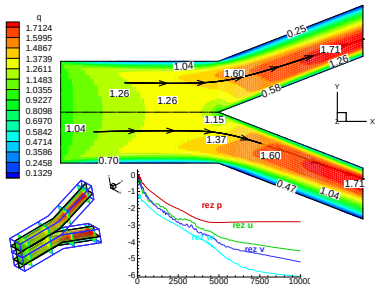


Fig. 10 Velocity isolines of 3D channel for non-Newtonian fluids

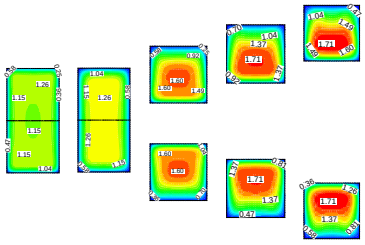

Fig. 11 Velocity isolines of 3D channel for Newtonian fluids

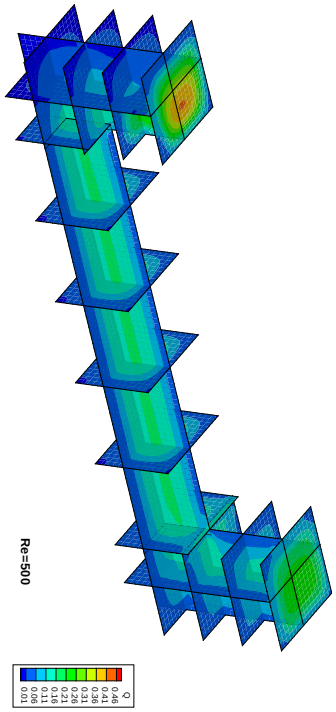


Fig. 12 Velocity isolines of 3D bypass for Newtonian fluids

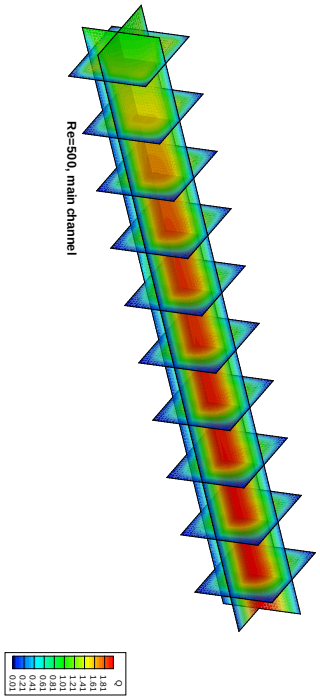


Fig. 13 Velocity isolines of 3D channel for Newtonian fluids

*ISBN 978-3-901608-32-2*  

This work was sponsered by Research Plan MSM 6840770010 and GA AS CR No. A 100190505

## 5 References

[1] R. J. LeVeque. *Numerical methods for conservation laws*. Birghüaser Verlag, Basel, Switzerland, 1990.

[2] A. J. Chorin. A numerical method for solving incompressible viscous flow problems. *Journal of Computational Physics*, 135:118–125, 1997.

[3] K. R. Rajagopal. Mechanics of non-newtonian fluids. In J. Nečas G. P. Galdi, editor, *Recent Developments in Theoretical Fluid Dynamics*, number 291 in Pitaman Research Notes in Math., pages 129–162. Longman & Technical, Essex, 1993.

[4] T. Yamaguchi T. Taylor. Three-dimensional simulation of blood flow in an abdominal aortic aneurysm, steady and unsteady flow cases. *J. Biomech. Engrg.*, 116:89–97, 1994.

[5] K. Kozel R. Keslerová. Numerical solution of incompressible laminar flows. In *Proc. The 13th International Conference on Fluid Flow Technologies CMFF'06*, Budapest, Hungary, September 2006.

[6] K. Kozel R. Keslerová and V. Prokop. Numerical solution of newtonian flow in bypass and non-newtonian flow in branching channels. In *Proc. of Programs and Algorithms of Numerical Mathematics 13*, pages 137–142, Prague, Czech Republic, May 28-31 2006. Mathematical Institute Academy of Science of the Czech Republic.

[7] E. Turkel A. Jameson, W. Schmidt. Numerical solution of the euler equations by finite volume methods using runge-kutta time-stepping schemes. *AIAA Paper 1981-1259, 14th Fluid and Plasma Dynamic Conference, June 23-25, Palo Alto, California*, 1981.

[8] K. Kozel R. Dvořák. *Mathematical Modelling in Aerodynamics*. CTU Prague, Prague, Czech Republic, 1996.

 